*Dipsikha Bhattacharya**

Adamas University, Department of Chemistry, School of Basic and Applied Sciences, Kolkata, India

Scientific paper
ISSN 0351-9465, E-ISSN 2466-2585
https://doi.org/10.62638/ZasMat1041

Zastita Materijala 65 (1)
63 - 72 (2024)

Development of hyaluronate tethered magnetic nanoparticles for targeted anti-cancer drug delivery

ABSTRACT

Despite the tremendous progress in understanding the molecular basis of the disease, cancer still remains one of the leading causes of deaths. Recently, advances in nanotechnology are rapidly enabling the development of novel, multifunctional materials with combined cancer specific targeting, therapeutic and diagnostic functions within a single nanocomplex (NP) that address the shortcomings of traditional disease diagnostic and therapeutic agents. Among the myriad of nanocarriers, magnetic nanoparticles (MNPs) have sparked extensive promise as novel theranostic applications as these MNPs can be directly targeted to the diseased cells with effective therapeutic efficiency. For this, these MNPs should be modified with some highly biocompatible polymers (specially polysaccharides) exhibiting the cancer targeting properties that can strongly interact with receptors expressed on the target cancer to facilitate accurate detection of the specific cancer and enhanced delivery to the target site while reducing unintended tside effects. Over the last few years, many groups have reported hyaluronic acid (HA) as the targeting agent as it directly delivers targeted MNPs to CD44 overexpressed cancer cells. In most of the cases, doxorubicin (DOX) has been used as the anticancer drug as it is largely utilized for treating a broad spectrum of cancers. In our work, we have designed a novel, intravenously injectable, CD44 receptor targeted MNP formulation, where the HA moiety of MNPs facilitate easy detection of cancer cells via receptor specific interactions, DOX can regress the cancer cells with simultaneous imaging efficacy. This theranostic MNPs led to the formation of novel nanoformulation, capable of performing concomitant detection, regression and imaging in in vitro CD44 over expressing cancer cells.

Keywords: *Multifunctional, MNP, Hyaluronic acid, Doxorubicin, CD44.*

1. INTRODUCTION

From last few decades, cancer, a complex, multifactorial disease are threatening human health by causing high mortality and recurrence rates [1]. The major drawbacks in chemotherapy are the poor intratumoral drug penetration and distribution, which can lead to serious off-target side effects and toxicities[2]. Another associated challenge in chemotherapy is the development of multidrug resistance (MDR) by tumor cells, which also reduced efficacy of drugs[3,4]. Therefore, it's important to create new methods for the precise identification of early-stage cancer and for targeted therapies that can only treat cancer with high dosages of lethal medications with minimal cytotoxicity to normal cells [5,6]. Recently nanotechnology provides an alternative strategy to overcome MDR by adopting various conceivable approaches to solve this issue. The increased permeability and retention (EPR) effect has been used to demonstrate that nanoparticles can passively accumulate in malignancies [7,8]. Among many multifunctional nanomedicines, magnetic nanoparticles (MNPs) have emerged as promising multifunctional nanoprobes because of their enhanced capability of delivering therapeutic agents (therapeutic drugs, DNA and small interfering RNA) to the targeted lesions along with their MR based diagnostic imaging efficiency [9-11]. Currently, a huge research impetus has been introduced to fabricate actively targeted MNPs with multiple imaging, detection and delivery functions through conjugating cancer specific “targeting” molecule to the surface of MNPs [12]. Many

*Corresponding author: Dipsikha Bhattacharya
E-mail: dipsikha.chem@gmail.com
Paper received: 28. 09. 2023.
Paper accepted: 20. 10. 2023.
Paper is available on the website: www.idk.org.rs/journal

molecular targeting agents such as various antibodies, peptides, naturally occurring polysaccharides, folic acid (FA) have been used in targeted drug delivery systems [13,14]. Among the natural polymers as cancer specific targeting agents, anionic glycosoaminoglycans such as hyaluronic acid (HA), its nonsulfated form has attracted striking interest not only due to their biodegradability, lower toxicity but also their contribution to the formation of extracellular constituent of connective tissues [15,16]. The main target molecule of HA is the antigen CD44 It is a breast cancer cell-surface glycoprotein antigen and is well known for its particular affinity for hyaluronic acid (HA) [17,18]. It is a multipurpose cell-surface molecule that has a role in the pathological characteristics of cancer cells, including cell proliferation, differentiation, migration, angiogenesis, and chemokines. Additionally, CD44 is known to be a marker for cancer stem cells, a subpopulation of cancer cells with the ability to self-renew. Hence, HA has been frequently utilized as a targeting moiety to detect CD44 receptors, which are available at low levels on epithelial, hematopoietic and neuronal cells and at elevated levels in various carcinomas, melanomas, lymphomas, colorectal, and lung tumor cells [15]. In recent times, the field of self-assembled HA carriers with CD44 targeting efficacy has attracted emerging attention as these nanocarriers can imbibe both the hydrophobic and hydrophilic therapeutics exploiting their amphiphilic nature [19-24]. In most of the cases, doxorubicin (DOX) molecules has been used as the anticancer drug as it is largely utilized for treating a broad spectrum of cancers. The main purpose of the present work is to develop a CD44 targeted HA-tethered nanotherapeutics with combined cancer specific targeting, diagnostic imaging and therapeutic efficiency for cancer specific drug delivery and noninvasive treatment monitoring. In order to overcome the intricate modification steps, we have prepared targeted DOX entrapped HA tethered MNPs where simple electrostatic interactions as well as chemical conjugation (as represented in Figure 1) was adopted for conjugating amine functionalities of Polyethylene imine (PEI) stabilized MNPs with carboxyl groups of HA groups. The DOX molecules are entrapped inside the self-assembled HA-MNP nanoparticles by the combined hydrophobic and the ionic interactions to construct a CD44 receptor targeted nanoprobes with targeting, imaging and therapeutic property. This theranostic pro drug with HA, DOX, Fluorescent dyes and MNPs led to the formation of novel nanoformulation, capable of performing concomitant detection, regression and imaging in in vitro CD44 over expressing cancer cells. These CD44 targeted formulations were extensively evaluated in CD44 over expressing cancer cells while extensive crosschecking with normal cells.

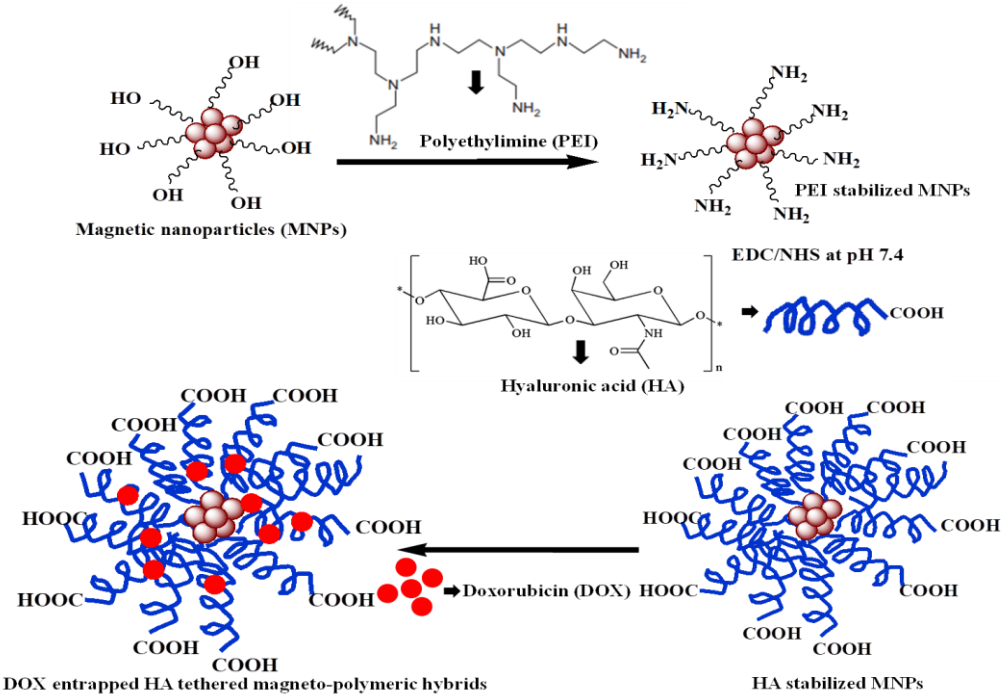

Figure 1. Schematic representation of synthesis of PEI functionalized MNPs followed by targeting with HA and DOX loading

Slika 1. Šematski prikaz sinteze PEI funkcionalizovanih MNP-a nakon čega sledi ciljanje sa HA i DOX opterećenjem

2. MATERIALS AND METHODS

2.1. Materials

Ferric chloride ($FeCl_3$), ferrous sulphate ($FeSO_4.7H_2O$), branched poly-(ethylenimine) (PEI, 25 kDa), hyaluronic acid (HA), N-hydroxy-succinimide (NHS), and 1-[3-(dimethylamino)-propyl] The following items were acquired from Sigma-Aldrich Chemicals in the United States: 3-ethyl carbodiimide hydrochloride (EDC), rhodamine isothiocyanate (RITC), doxorubicin, 4-6-diamidino-2-phenylindole (DAPI), propidium iodide (PI), RNase, and 3-(4,5-dimethylthiazol-2-yl)-2,5- Vacuum distillation was used to clean up commercially available dimethyl sulfoxide (DMSO) and N, N-dimethyl formamide (DMF), then dried 1, 4-dioxane was distilled over salt. We bought chloroform ($CHCl_3$) from Merck in Germany. Minimum essential medium (MEM) and foetal bovine serum were purchased from Hyclone in the United States and Himedia in India, respectively.

2.2. Methods

Synthesis of amine functionalized PEI-MNPs and HA targeted PEI-MNPs

Highly hydrophilic, biocompatible MNPs were synthesized using the standard controlled co-precipitation approach of using Fe^{2+} and Fe^{3+} (1:2 ratio) in presence of branched PEI according to our previously reported procedure[25,26]. In brief, a mixture of 0.324 g of $FeCl_3$ and 0.278 g of $FeSO_4.7H_2O$ were dissolved in 40 ml deoxygenated Milli-Q water containing 2 mg/ml of branched PEI in a three neck flask with a magnetic stirrer and an argon flow. To this, ammonium hydroxide (5 ml) was added drop wise and the mixture was stirred for 4 h at 70ºC. After completion of the reaction, these PEI-MNPs were recovered using magnetic separation, dialysis followed by freeze drying. Hyaluronic acid tethering to PEI-MNPs was carried out via EDC/NHS chemistry according to a reported procedure with little modification [27]. In a typical synthesis, a total of 100 mL of PBS, 0.15 g of HA, 0.1 g of EDC.HCl, and 0.6 g of NHS were added. Dilute NaOH was used to keep the pH between 8 and 10. Using EDC (100 mg, 0.48 mM) and NHS (56 mg, 0.48 mM) for 4 hours in the dark, the carboxyl group was activated. Subsequently, it was mixed with the aqueous dispersion of 150 mg of PEI-MNPs, and the final mixture was agitated overnight at RT. The HA-PEI-MNPs were finally retrieved after being magnetically concentrated, multiple times washed with Milli Q water, and PBS.

Development of anticancer drug entrapped HA-PEI-MNPs

After the successful development of MNP nanocarriers, doxorubicin (DOX), the anticancer drug, was entrapped inside these HA-PEI-MNPs with the weight ratio of 1:10. The red-colored solution was gently swirled for 36 hours at 25ºC in the dark. The resultant solution was then dialyzed against double distilled water while being stirred for 24 hours and having at least five water changes to get rid of undesirable components. To get DOX, the dialyzed solution was lyophilized in a speed vacuum for 24 hours. To get DOX, the dialyzed solution was lyophilized in a speed vacuum for 24 hours loaded HA-PEI-MNPs [28]. For evaluation of the loading and entrapment of the drug, 2 mg amount of DOX loaded nanoparticles were dissolved in 10 ml of Milli-Q water under stirring condition and absorbance of the drug was checked using standard UV-Vis and Fluorescence microscopy. It was degraded for 24 h in 10 ml of PBS: water mixture (1:1) under gentle shaking and the absorbance of the solution was measured at 480 nm. The amount of DOX entrapped inside this MNPs was determined using a previously drawn calibration curve of the drug using different concentrations. All the measurements were performed in triplicate.

$$\textit{Drug Loading } (DL) = \frac{DOX \times 100}{MNP + DOX} \qquad (1)$$

Entrapment Efficiency

$$(EE) = \frac{\textit{Amount of actual DOX loaded in MNPs}}{\textit{Amount of total DOX taken for entrapment}} \qquad (2)$$

To investigate the release of DOX, 10 mg of DOX-HA-PEI-MNPs were dispersed in 10 ml PBS solution and was placed in a dialysis bag at different pH values i.e. 7.4 (molecular weight cut-off of 12 kDa). The bags were suspended in 50 ml PBS solution at pH 7.4 and shaken for 5 days at 200 rpm. At selected time intervals, 1 ml of the sample was taken and replaced by an equal volume of fresh PBS. By spectrophotometrically analysing the solution's absorbance at 480 nm collected at predetermined intervals, the amount of released DOX was determined [26]. After being measured, and the samples that were obtained for sampling were added back to the receiver solution. A standard curve of a free drug solution was used to calculate the percentage of released drug. Three independent experiments' means and standard deviations were used to express the data.

Preparation of RITC labelled HA-PEI-MNPs (fluorescent conjugates of 1 and 2).

For the fluorescent labelling, a fraction of the previously stated HA-Poly-MNPs were covalently coupled using the amine groups with the highly fluorescent molecule rhodamine isothiocyanate (RITC) for the fluorescent labelling according to the previous reported literature [26].

The characterization of nanoparticles

Transmission electronic microscopy was used to observe the nanoparticles' size and form (TEM, JEOL-2100). The nanoparticles were dissolved in deionized water and subjected to a 10-minute ultrasonic process for the TEM investigation. The solution was then dropped onto a copper grip that had been carbon-coated before the pictures were taken and air-dried [29]. Image J software was used to analyse the average particle size. The MNPs' alteration was controlled by FTIR spectra in the range 500–4000cm^{-1}.

Cell lines and cytotoxicity studies.

The biocompatibility of the HA-PEI-MNPs and cytotoxicity of DOX–HA–PEI-MNPs was evaluated by a standard MTT [3-(4, 5-dimethylthiazol-2-yl)-2,5-diphenyltetrazolium bromide] assay. Two types of cells cultivated for in vitro experiments were A549 (Lung Carcinoma Cell Line for adenovirus) and HaCaT (immortalized human keratinocyte), which were acquired from the National Centre for Cell sciences (NCCS), Pune, India.Trypsinized cells were adjusted to a concentration of 1×10^5 cells per ml and plated in 96 well flat bottom culture plates for the cytotoxicity assay. (180 ml per well) and were incubated with DOX–HA–PEI-MNPs for 24 h at 37ºC in a humidified 5% CO_2 incubator [30]. Cell toxicity was measured by the MTT colorimetric procedure. Mean and standard deviation for the triplicate wells were reported.

Intracellular uptake studies by Confocal imaging and Prussian blue staining

The internalization and intracellular distribution of HA-PEI-MNPs were observed by fluorescence microscopic imaging. The PEI-MNPs and HA-PEI-MNPs were incubated with A549 cells. The cells (1×10^6 cells/well) were treated with 1 mg/ml of nanoconjugates in the culture for 4 h, the culture media were removed, and the cells were washed three times with PBS. The cells were then stained with DAPI for 10 min at room temperature and observed by fluorescence microscopy [26]. For the concentration dependent uptake via Prussian Blue staining, 1×10^6 cells was seeded in each wells for 24 h and were incubated with 25µg/ml of non-targeted PEI-MNPs and dose dependent concentrations of 5, 10, 20 and 25 µg/ml of targeted HA-PEI-MNPs for 4h respectively. After the incubation period, these wells were washed with PBS to remove any free nanoparticles. Cells were fixed for 40 minutes using 4% paraformaldehyde (Sigma-Aldrich). The cells were washed three times with PBS, counterstained with neutral red (0.02%) (Sigma-Aldrich), and subsequently observed by an inverted optical microscope [31,32].

Cell cycle analysis.

For the evaluation of the therapeutic efficacy of the DOX–HA–PEI-MNPs, time dependent cell-cycle analysis was performed in A549 cells. Cells (1×10^5) were treated with 10 µg free DOX, 25 µg HA-PEI-MNPs and the same concentrations of DOX-HA-PEI-MNPs for 0 hr, 30 min, 1 hr and 2 hrs at 37ºC. Cells were harvested and fixed in ethanol with a 70% alcohol content. The cells were then washed with ice-cold PBS (10 mM, pH 7.4), resuspended in 200 l of PBS, and incubated at 37 oC for 1 h in the dark with 20 l of DNA intercalating dye PI (1 mg/ml) and 20 l of DNAase free RNase. The hypochromic sub-diploid staining characteristics of the cells were used to identify apoptotic cells. Using a Becton-Dickinson FACS Calibur Flow Cytometer and Cell Quest software, the DNA histogram was examined to determine the distribution of cells in various cell-cycle phases.

DAPI staining for nuclear morphology study.

For visualization of A549 cells, the cell nucleus was stained with DAPI. The DAPI staining was performed to corroborate the apoptotic effect of DOX entrapped MNPs on A549 cells. For this, A549 cells were treated with HA-PEI-MNPs (control set) and (5, 10, 20 and 25 µg/ml) of DOX–HA–PEI-MNPs for 24 h at 37ºC. After this, cells were fixed with 3.7% formaldehyde for 15min, permeabilized with 0.1 percent Triton X-100 and dyed for 5 minutes at 37 degrees with 1 g/ml DAPI. After being cleaned with PBS, the cells were analysed using fluorescence microscopy (Olympus IX 70).

Statistical Analysis

One-way ANOVA was used to assess the statistical significance of differences (p 0.05) between the groups tested.

3. RESULTS AND DISCUSSIONS

HA-MNPs with superparamagnetic properties are synthesised from the step up chemistry of PEI-MNPs followed by the successful modification with Hyaluronic acid which is represented in Scheme 1. First, NH_2 functionalized highly stable, water-dispersible MNPs were synthesized through a standard co-precipitation technique using PEI as the stabilizing as well as surface anchoring agent.

Further, HA was used as a CD44 receptor specific targeting agent to introduce targeting efficacy on the PEI-MNPs and the carboxylic acid groups in HA molecules were covalently conjugated with the ample NH_2 functionalities of PEI-MNPs through standard carbodimide activation approach. Therefore, the carboxyl groups of the HA molecules were conjugated to the amine group on the surface of NH_2-MNPs via the formation of amide bonds (HA-MSNs) [33,34]. Both of these PEI-MNPs and HA-PEI-MNPs were labelled with RITC by covalent linking utilizing some of the residual surface amine groups [25]. The structure of PEI-MNPs and HA-PEI-MNPs was observed by transmission electron microscopy (TEM) analysis. As indicated in Figure 2(A-B), it was confirmed that before modification through HA, the size of the PEI-MNPs were in between 5-7 nm whereas after modification with high molecular weight HA, these HA-PEI-MNPs showed a size enhancement around 7 nm showing the size in the range of 15-17 nm. It authenticates their successful modification with PEI as well as HA as shown in Figure 2(A-B). The particle sizes of these functionalized MNPs were also checked by Dynamic Light Scattering technique i.e DLS. The hydrodynamic diameters (HDs) of these PEI-MNPs and HA-PEI-MNPs were observed at 85±10 nm and 205±10 nm (Table 1) with poly dispersity index (PDI) 0.25 and 0.28 of indicating larger diameters observed from TEM. This discrepancy is due to the fact that TEM measures the size of the NP core under vaccum, while the hydrodynamic diameter is a measure of the size of the core and the total hydrated coating in solution[35].

The surface charges of these nanoconjugates also show the +45.7 and -27.8 mV confirming the successful functionalization with NH_2 groups of PEI and –COOH groups of HA molecules. The decrease of zeta potential of the MNPs from +45.7 to -27 indicates the free amine groups of PEI-MNPs should be protonated and hence positive charged at neutral pH while after modification with HA, as HA is negatively charged –COOH groups and –CONH groups due to covalent bonding, this rendered HA-PEI-MNPs bearing negative zeta potential [36,37]. The successful functionalization with HA was confirmed by Fourier transform infrared (FTIR) spectroscopy. The FTIR spectra of HA-PEI-MNPs (Figure 2D) have shown all the peaks at 3470 cm^{-1}, 2936 cm^{-1}, 2856 cm^{-1}, 1358 cm^{-1}, 1230 cm^{-1}, 1057 cm^{-1} and 560 cm^{-1} indicating the presence of NH2, O-H, C-H, C-O, NH-CO and Fe-O stretching vibrations, respectively [38].

Table 1. Hydrodynamic (HD) size and zeta potential of the PEI-MNPs and HA-PEI-MNPs at physiological pH.

Tabela 1. Hidrodinamička (HD) veličina i zeta potencijal PEI-MNP i HA-PEI-MNP pri fiziološkom pH.

Nanoparticles	Size (nm)	Poly dispersity index (PDI)	Zeta potential (mV)
PEG-NH_2-MNPs	85±10	0.25	+45.7
HA-PEI-MNPs	205±6	0.28	-27.8

3.1. Therapeutic efficiency, Potential Cytotoxicity and Receptor Mediated Internalization analysis

Despite the powerful anti-cancer actions of doxorubicin (DOX), its non-specific side effects led to the creation of DOX loaded HA targeted nanocarriers to enable tumor-specific targeting. According to UV-vis spectrophotometry used in this investigation, the DOX loading and entrapment efficiency of DOX-HA-PEI-MNPs was around 6.2 percent and 82 percent [26,39]. According to a prior publication, DOX molecules can be loaded inside nanocarriers using both covalent pH-sensitive bonding and hydrophobic/ionic interactions [40-42]. In our situation, the combination hydrophobic and hydrogen bonding interactions between DOX molecules led to the entrapment of DOX in HA-PEI-MNPs. and carboxyl groups of HA-PEI-MNPs as previously reported from our group [26]. As shown in Figure 2C, the release of DOX molecules from DOX-HA-PEI-MNPs at pH 7.4 shows a sustained release of 25% within 24 h indicating the successful entrapment as well as sustained release of therapeutics at physiological pH.

From the cytotoxicity assay as shown in Figure 2(E-F), the cellular toxicity values of DOX-HA-PEI-MNPs along with free DOX molecules were examined in healthy HaCaT and target cancer cells (A549 cells: high CD44 expression) for 24 h with cell proliferation kit. As HaCaT cells has low CD44 expression, DOX-HA-PEI-MNPs shows almost 80% cell viability in comparison to free drug in normal HaCaT cells while in A549 cells with high CD44 expression, DOX-HA-PEI-MNPs indicates higher cytotoxicity compared to free drug molecules. Thus, due to the targeted internalization in A549 cells, the DOX-HA-PEI-MNPs shows enhanced toxicity indicating their efficiency over bulk DOX molecules. To authenticate the targeted CD44 receptor mediated internalization of RITC-HA-PEI-MNPs labelled over RITC-PEI-MNPs, confocal laser scanning microscopy was used and these nanoconjugates were incubated with A549 cells for 4 h which was shown in Figure 3(A-B). Compared with the internalization of RITC-PEI-MNPs demonstrated in Figure 3(A), HA targeted nanoconjugates (as shown in Figure 3B) showed

enhanced red fluorescence intensity indicating higher internalization of RITC-HA-nanoconjugates due to the CD44 receptor mediated endocytosis of HA-PEI-MNPs [43,44]. The dose dependent intracellular uptake of HA-PEI-MNPs was investigated using Prussian Blue staining in shown in Figure 3(C-G). According to the images shown, the HA-PEI-MNPs show enhanced cell uptake when same concentrations of A549 cells was incubated with increasing concentrations from 5, 10, 20 and 25 µg/ml Figure 3(D-G). It was evident that due to the CD 44 receptor mediated internalization, HA-PEI-MNPs exhibited enhanced intracellular uptake as compared to PEI-MNPs of the same concentration.

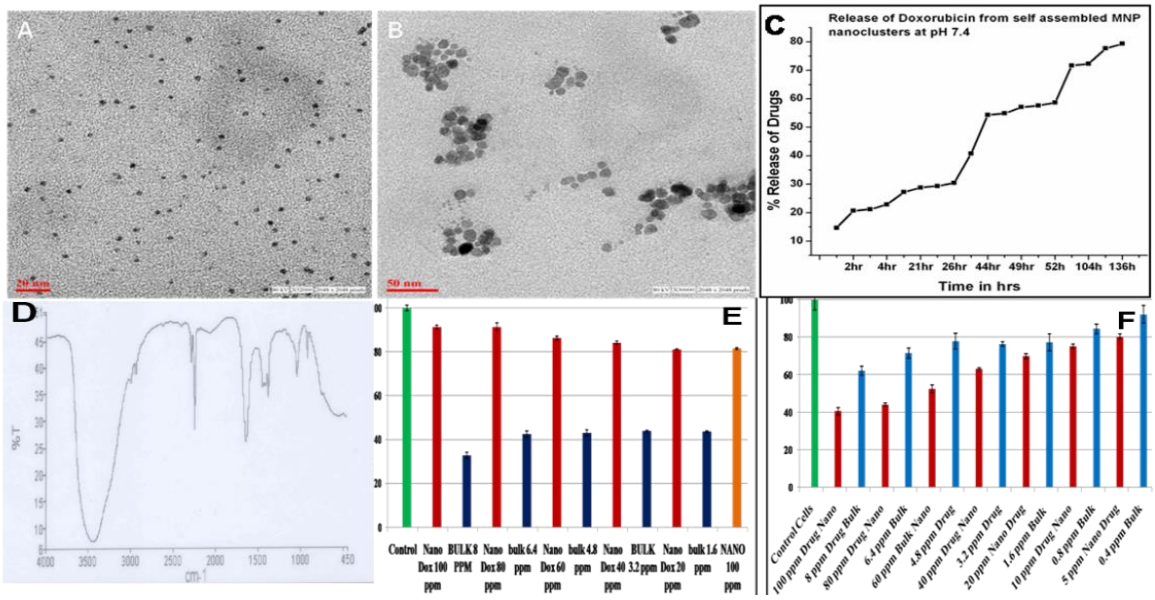

Figure 2. (A-B) TEM images of PEI-MNPs and HA-PEI-MNPs, C) DOX release from DOX-HA-PEI-MNPs, D) FT-IR spectrum of HA-PEI-MNPs. (E-F) MTT assays of DOX-HA-PEI-MNPs in HaCaT and A549 cells

Slika 2. (A-B) TEM slike PEI-MNP i HA-PEI-MNP, C) Oslobađanje DOX iz DOX-HA-PEI-MNP, D) FT-IR spektar HA-PEI-MNP, (E-F) MTT testovi DOX-HA-PEI-MNP u HaCaT i A549 ćelijama

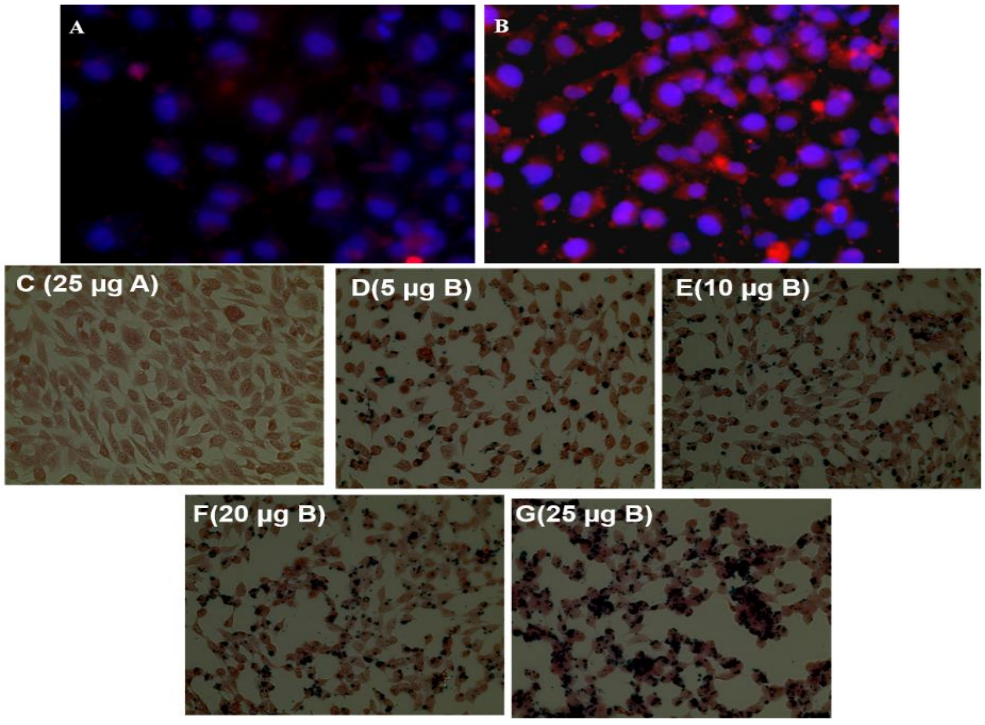

Figure 3. (A-B) Intracellular uptake of PEI-MNPs and HA-PEI-MNPs in A549 cells. (C-G) Intracellular uptake by Prussian Blue Staining of C) 25 µg/ml of PEI-MNPs D) to G) 5, 10, 20 and 25 µg/ml of HA-PEI-MNPs

Slika 3. (A-B) Intracelularno preuzimanje PEI-MNP i HA-PEI-MNP u A549 ćelijama. (C-G) Intracelularno preuzimanje pruskom plavim bojenjem od C) 25 µg/ml PEI-MNP D) do G) 5, 10, 20 i 25 µg/ml HA-PEI-MNP

Propidium iodide (PI) and DAPI staining have been used to analyse the cell cycle and undertake DNA fragmentation studies, or apoptosis studies, to further assess the anti-proliferative effect of DOX-HA-PEI-MNPs on A549 cells. From the DNA fragmentation study using increasing concentration of DOX–HA-PEI-MNPs (5, 10, 20 and 25 µg/ml) as represented in Figure 4(A-B), it was indicative that with increasing concentration there was substantial nuclei fragmentation, including membrane blebbing, condensed nuclei, and the development of apoptotic bodies.

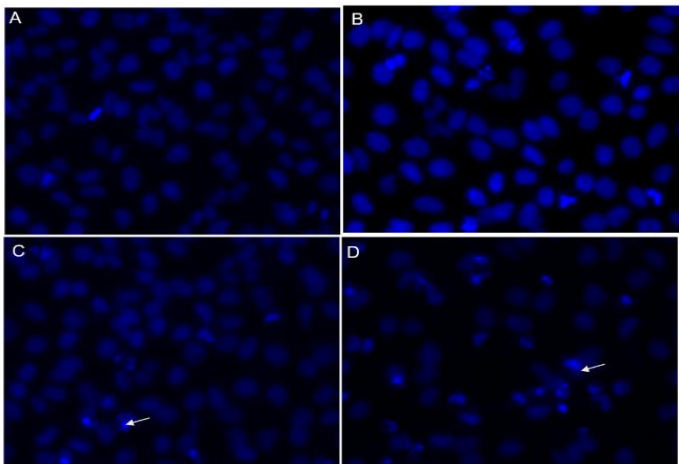

Figure 4. (A-D) DOX-HA-PEI-MNPs were used to evaluate apoptosis by examining the morphological changes in cell nuclei using fluorescence microscopy following DAPI labelling. For 24 hours, DOX-HA-PEI-MNPs were administered to A549 cells at concentrations of (A) 5 g/ml, (C) 10 g/ml, (D) 20 g/ml, and (E) 25 g/ml. Apoptotic nuclei are shown by arrows

Slika 4. (A-D) DOX-HA-PEI-MNP-ovi su korišćeni za procenu apoptoze ispitivanjem morfoloških promena u ćelijskim jezgrima korišćenjem fluorescentne mikroskopije nakon obeležavanja DAPI. Tokom 24 sata, DOX-HA-PEI-MNP su davani ćelijama A549 u koncentracijama od (A) 5 g/ml, (C) 10 g/ml, (D) 20 g/ml i (E) 25 g/ ml. Apoptotična jezgra su prikazana strelicama

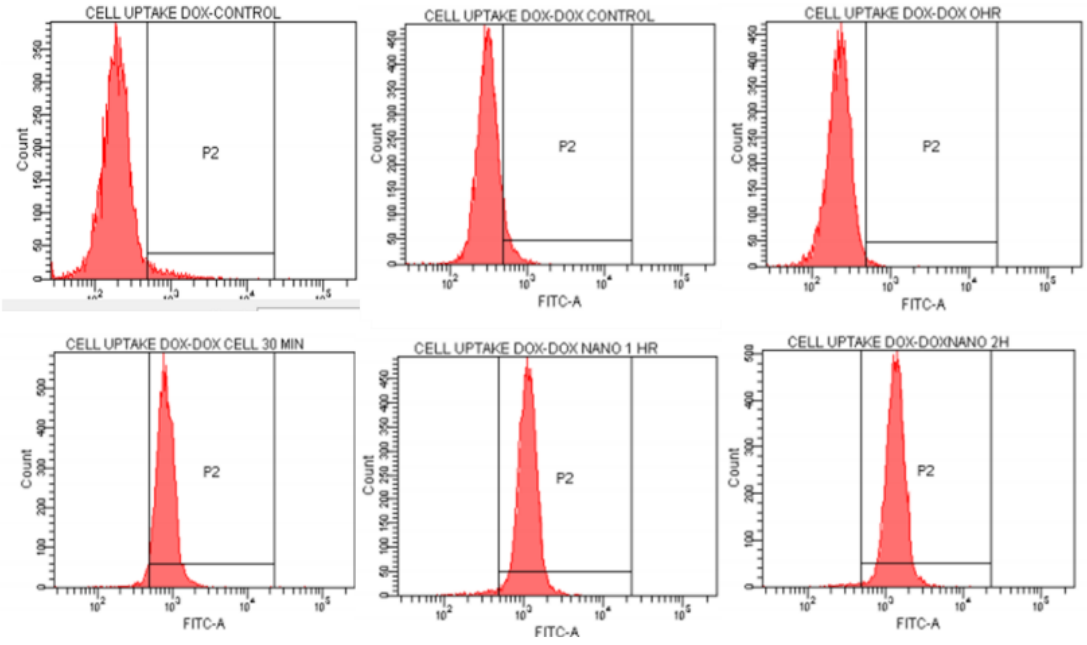

Figure 5. Flow-cytometric analysis of cell cycle phase distribution. Distribution of A549 cells treated with (A) HA-targeted nanoparticles (B) DOX only (C) 25 µg/mL of DOX-HA-MNPs for 0 hr (D) 25 µg/mL of DOX-HA-MNPs for 0.5 hr (E) 1 hr (F) 2 hrs

Slika 5. Protočna citometrijska analiza distribucije faza ćelijskog ciklusa. Distribucija ćelija A549 tretiranih sa (A) HA ciljanim nanočesticama (B) samo DOX (C) 25 µg/mL DOX-HA-MNP tokom 0 sati (D) 25 µg/mL DOX-HA-MNP tokom 0,5h (E) 1 sat (F) 2h

It was also evident that as the concentration of DOX-Poly-FA-MFNPs increased, the number of apoptotic nuclei increased as well (apoptotic nuclei shown by arrow in the Figure 4).This observation was fully supported by cell cycle analysis shown in Figure 5 where only HA-PEI-MNPs with highest concentration (25 µg/ml) has no apoptotic effect while increasing concentrations of DOX–HA-PEI-MNPs showed the maximum cell intensification at the G2/M phase [45], exhibiting cell cycle arrest in the same phase. Therefore, these DOX-HA-PEI-MNPs inhibited the growth of A549 cells by arresting cell cycle progression at the G2/M phase and followed to apoptosis or cell death.

4. CONCLUSIONS

In summary, we successfully fabricated DOX entrapped CD 44 receptor targeted HA-PEI-MNPs with combined cancer specific targeting and optical imaging by a facile preparation method. TEM images showed that these HA targeted nanoconjugates are highly dispersed and as they are intricately designed for the drug delivery applications, they should especially be taken up by cancer cells as opposed to normal cells. According to in vitro biological investigations, the DOX-HA-PEI-MNPs can deliver a single nanoconstruct with exceptional efficacy for locating and eliminating cancer cells.The DOX-HA-PEI-MNPs could efficiently deliver DOX to the tumor tissues, and gradually destroy CD44 receptor expressing cells compared to the free drug. Although further studies are needed, the various studies described in this manuscript indicate that the DOX-HA-PEI-MNPs represent an attractive nanocarrier that should have great potential for the treatment of cancer.

Acknowledgements

The authors are grateful to DST Nano Mission as well as Adamas University for providing financial support for this work.

5. REFERENCES

[1] M.Maluccio, A.Covey (2012) Recent progress in understanding, diagnosing, and treating hepato-cellular carcinoma; CA Cancer J Clin., 62, 394-399.

[2] S.Senapati, A.K.Mahanta, K.Sunil, P.Maiti (2018) Controlled drug delivery vehicles for cancer treatment and their performance; Signal Transduct Target Ther., 3, 7-26.

[3] L.Gan, L.Zhenjiang, S.Chao (2018) Obesity linking to hepatocellular carcinoma: A global view; Biochim Biophys Acta Rev Cancer., 1869, 97-102.

[4] C.Sun, J.S.Lee, M.Zhang (2008) Magnetic nanoparticles in MR imaging and drug delivery; Adv. Drug Deliv. Rev., 60, 1252-1265.

[5] M.E.Davis, Z.Chen, D.M.Shin (2008) Nanoparticle therapeutics: an emerging treatment modality for cancer; Nat. Rev. Drug Discov., 7, 771-782.

[6] O.Veiseh, J.W.Gunn, M.Zhang (2010) Design and fabrication of magnetic nanoparticles for targeted drug delivery and imaging; Adv. Drug Deliv.Rev., 62, 284-304.

[7] H.Maeda, J.Wu, T.Sawa, Y.Matsumura, K.Hori (2000) Tumor vascular permeability and the EPR effect in macromolecular therapeutics: a review; J Control Release; 65, 271-284.

[8] H.Maeda, T.Sawa, T.Konno (2001) Mechanism of tumor-targeted delivery of macromolecular drugs, including the EPR effect in solid tumor and clinical overview of the prototype polymeric drug SMANCS; J. Control Release., 74, 47-61.

[9] J.W.M.Bulte, D.L.Kraitchman (2004) Iron oxide MR contrast agents for molecular and cellular imaging; NMR Biomed., 17, 484-499.

[10] J.H.Lee, Y.M.Huh, Y.Jun, J.Seo, J.Jang, H.T.Song, S.Kim, E.J.Cho, H.G.Yoon, J.S.Suh, J.Cheon (2007) Artificially engineered magnetic nanoparticles for ultra-sensitive molecular imaging. Nat. Med., 13, 95-99.

[11] Y.Pineiro, M.González Gómez, L. de Castro, A. Arnosa Prieto, A.García, P.S.Gudiña, R.Puig, J. Teijeiro, C.Yáñez-Vilar, S.J.Rivas (2020) Hybrid Nanostructured magnetite nanoparticles: from bio-detection and theragnostics to regenerative medicine. Magnetochemistry, 6, 4-31.

[12] A.Angelopoulou, A.Kolokithas-Ntoukas, C.Fytas, K. Avgoustakis (2019) Folic Acid-Functionalized, Condensed Magnetic Nanoparticles for Targeted Delivery of Doxorubicin to Tumor Cancer Cells Overexpressing the Folate Receptor. ACS Omega, 4, 22214-22227.

[13] S.D.Jo, S.H.Ku, Y.Y.Won, S.H.Kim, I.C.Kwon (2016) Targeted Nanotheranostics for Future Personalized Medicine: Recent Progress in Cancer Therapy; Theranostics, 6, 1362-1377.

[14] Z.Fang, X.Li, Z.Xu, F.Du, W.Wang, R.Shi, D.Gao (2019) Hyaluronic acid-modified mesoporous silica-coated superparamagnetic Fe3O4 nanoparticles for targeted drug delivery; International Journal of Nanomedicine, 14, 5785-5797.

[15] L.J.Lapcik, L.Lapcik, S.S.De, J.Demeester, P. Chabrecek (1998) Hyaluronan Preparation, Struc-

ture, Properties, and Applications; Chem. Rev., 98, 2663-2684.

[16] B.P.Toole (2004) Hyaluronan: from extracellular glue to pericellular cue; Nat. Rev. Cancer, 4, 528-539.

[17] Y. Lee, H. Lee, Y.B. Kim, J. Kim, T. Hyeon, H. Park, P.B. Messersmith, T.G. Park (2008) Bioinspired Surface Immobilization of Hyaluronic Acid on Monodisperse Magnetite Nanocrystals for Targeted Cancer Imaging; Adv Mater, 20, 4154-4157.

[18] H.Ponta, L.Sherman, P.A.Herrlich (2003) CD44: from adhesion molecules to signalling regulators; Nat Rev Mol Cell Biol, 4, 33-45.

[19] H.J.Chung, H.Lee, K.H.Bae, Y.Lee, J.Park, H.Cho, J.Y.H.Park, R.Langer, D.Anderson, T.G.Park (2011) Facile Synthetic Route for Surface-Functionalized Magnetic Nanoparticles: Cell Labelling and Magnetic Resonance Imaging Studies. ACS Nano, 5, 4329-4336.

[20] K.Y.Choi, K.H.Min, J.H.Na, K.Choi, K.Kim, J.H. Park, I.C.Kwon, S.Y.Jeong (2009) Self-assembled hyaluronic acid nanoparticles for active tumor targeting; J Mater Chem, 19, 106-114.

[21] H.J. Cho, H.Y. Yoon, H. Koo, S.H. Ko, J.S. Shim, J.H. Lee, K. Kim, I.C. Kwon, D.D. Kim (2011) Self-assembled nanoparticles based on hyaluronic acid-ceramide (HA-CE) and Pluronic® for tumor-targeted delivery of docetaxel. Biomaterials, 32, 7181-7190.

[22] W. Park, K.S.Kim, B.C.Bae, Y.H. Kim, K. Na (2010) Cancer cell specific targeting of nanogels from acetylated hyaluronic acid with low molecular weight. Eur J Pharm Sci, 40, 367-375.

[23] T.Gong, Z.Dong, Y. Fu, T.Gong, L.Deng, Z.Zhang (2019) Hyaluronic acid modified doxorubicin loaded Fe_3O_4 nanoparticles effectively inhibit breast cancer metastasis. J. Mater. Chem. B, 7, 5861-5872.

[24] L. Song, Z. Pan, H. Zhang, Y. Li, Y. Zhang, J. Lin, G. Su, L. Xie, Y. Li, Z. Ho (2017) Dually folate/CD44 receptor-targeted self-assembled hyaluronic acid nanoparticles for dual-drug delivery and combination cancer therapy. J Mater Chem B., 5, 6835-6846.

[25] D. Bhattacharya, M.Das, D.Mishra, I. Banerjee, S. K. Sahu, T. K Maiti, P. Pramanik (2011) Folate receptor targeted, carboxymethyl chitosan functionalized iron oxide nanoparticles: a novel ultradispersed nanoconjugates for bimodal imaging. Nanoscale, 3, 1653 -1662.

[26] D.Bhattacharya, B.Behera, S.K.Sahu, R. Ananthakrishnan, T.K.Maity, P.Pramanik (2016) Design of dual stimuli responsive polymer modified magnetic nanoparticles for targeted anti-cancer drug delivery and enhanced MR imaging. New J. Chem., 40, 545-557.

[27] B. Gupta, B.K. Poudel, H.B. Ruttala, S. Regmi, S. Pathak, M. Gautam, S. Jin, J.H. Jeong, H.G. Choi, S. K. Ku, C. S. Yong, J. O. Kim (2018) Hyaluronic acid-capped compact silica-supported mesoporous titania nanoparticles for ligand-directed delivery of doxorubicin. Acta Biomaterialia, 80, 364--377.

[28] S. Wang, J. Zhang, Y. Wang, M. Chen (2016) Hyaluronic acid-coated PEI-PLGA nanoparticles mediated co-delivery of doxorubicin and miR-542-3p for triple negative breast cancer therapy. Nanomedicine, 12, 411-420.

[29] K. Kim, K. Kim, J. H. Ryu, H. Lee (2015) Chitosan-catechol: a polymer with long-lasting mucoadhesive properties. Biomaterials, 52, 161-170.

[30] S. Wen, H. Liu, C. Hongdong, M. Shen, X. Shi (2013) Targeted and pH-responsive delivery of doxorubicin to cancer cells using multifunctional dendrimer-modified multi-walled carbon nanotubes. Adv. Healthcare Mater, 2, 1267-1276.

[31] A.M. Reddy, B.K. Kwak, H.J. Shim (2010) In vivo Tracking of Mesenchymal Stem Cells Labeled with a Novel Chitosan-coated Superparamagnetic Iron Oxide Nanoparticles using 3.0T MRI. J Korean Med Sci., 25, 211-219.

[32] J. Krejci, J. Pachernik, A. Hampl, P. Dvorak (2008) In vitro labelling of mouse embryonic stem cells with SPIO nanoparticles. Gen Physiol Biophys, 27, 164-173.

[33] J. Y. Jeong, E.H. Hong, S. Y. Lee, J.Y. Lee, J. H. Song, S. H. Ko, J. S. Shim, S. Choe, D. D. Kim, H.J. Ko, H. J. Cho (2017) Boronic acid-tethered amphiphilic hyaluronic acid derivative-based nanoassemblies for tumor targeting and penetration. Acta Biomater, 53, 414-426.

[34] M. Ashrafizadeh, S. Mirzaei, M.H. Gholami, F. Hashemi, A. Zabolian, M. Regi, K. Hushmandi, A. Zarrabi, N.H. Voelcker, A. Reza Aref, M. Hamblin, R. Varma, R. S. Samarghandian, S. Arostegi, I.J. Alzola, M. Prem Kumar, A.Thakur, V. K. Nabavi, N. Makvandi, P. Tay, F. R. Orive, (2021) Hyaluronic acid-based nanoplatforms for Doxorubicin: A review of stimuli-responsive carriers, co-delivery and resistance suppression. Carbohydrate Polymers, 272, 118491-118521.

[35] H.A. Chen, Y.J. Lu, B. S. Dash, Y. K. Chao, J. P. Chen (2023) Hyaluronic Acid-Modified Cisplatin-Encapsulated Poly(Lactic-co-Glycolic Acid) Magnetic Nanoparticles for Dual-Targeted NIR-Responsive Chemo-Photothermal Combination Cancer Therapy. Pharmaceutics., 15, 290-314.

[36] J. Dou, Y.Mi, S.Daneshmand, M.H.Majd (2022) The effect of magnetic nanoparticles containing hyaluronic acid and methotrexate on the expression of genes involved in apoptosis and metastasis in A549 lung cancer cell lines. Arabian Journal of Chemistry., 15,104307.

[37] H.C.Wu, T.W.Wang, S.Y.Hsieh, J.S.Sun, P.L.Kang (2016) Targeted Delivery of Hyaluronan-Immobilized Magnetic Ceramic Nanocrystals. J. Biomed. Nanotechnol, 12, 103-113.

[38] M.D.Zhao, J.L.Cheng, J.J.Yan, F.Y.Chen, J.Z. Sheng, D.L.Sun, J.Chen, J.Miao, R.J.Zhang, C.H. Zheng, H.F.Huang (2016) Hyaluronic acid reagent functional chitosan-PEI conjugate with AQP2-siRNA suppressed endometriotic lesion formation. Inter. J. Nanomed., 11, 1323-1336.

[39] Z.Chai, C.Teng, L.Yang, L.Ren, Z.Yuan, S. Xu, M. Cheng, Y.Wang, Z.Yan, C.Qin, X. Han, L.Yin

(2020) Doxorubicin delivered by redox-responsive Hyaluronic Acid–Ibuprofen prodrug micelles for treatment of metastatic breast cancer. Carbohydrate Polymers, 245, 116527-116545.

[40] Y.L.Su, J.Wang, H.Z.Liu (2002) Formation of a Hydrophobic Microenvironment in Aqueous PEO−PPO−PEO Block Copolymer Solutions Investigated by Fourier Transform Infrared Spectroscopy. J. Phys. Chem. B, 106, 11823-11828.

[41] S. Liu, Y.Zhao, M. Sen. Y. Hao, X. Wu, Y. Yao, Y. Li, Q. Yang. (2022) Hyaluronic acid targeted and pH-responsive multifunctional nanoparticles for chemo-photothermal synergistic therapy of atherosclerosis. J. Mater. Chem. B. 10, 562-570.

[42] Z. Luo, Y.Dai, H.Gao (2019) Development and application of hyaluronic acid in tumor targeting drug delivery. Acta Pharmaceutica Sinica B., 9, 1099-1112.

[43] H.Urakawa, S.Tsukushi, H.Sugiura (2014) Neoadjuvant and adjuvant chemotherapy with doxorubicin and ifosfamide for bone sarcomas in adult and older patients. OncolLett., 8, 2485-2488.

[44] X.Pang, Z.Lu, H.Du, X.Yang, G.Zhai (2014) Hyaluronic acid-quercetin conjugate micelles: Synthesis, characterization, in vitro and in vivo evaluation. Colloids Surf B Biointerfaces., 123, 778-786.

[45] Y.H.Ling, A.K. el-Naggar, W.Priebe, R.Perez-Soler (1996) Cell cycle-dependent cytotoxicity, G2/M phase arrest, and disruption of p34cdc2/cyclin B1 activity induced by doxorubicin in synchronized P388 cells. Mol. Pharmacol., 49, 832-841.

IZVOD

RAZVOJ MAGNETNIH NANOČESTICA VEZANIH HIJALURONATOM ZA CILJANU ISPORUKU LEKOVA PROTIV RAKA

Uprkos ogromnom napretku u razumevanju molekularne osnove bolesti, rak i dalje ostaje jedan od vodećih uzroka smrti. Nedavno, napredak u nanotehnologiji ubrzano omogućava razvoj novih, multifunkcionalnih materijala sa kombinovanim ciljanim, terapeutskim i dijagnostičkim funkcijama za rak u okviru jednog nanokompleksa (NP) koji se bavi nedostacima tradicionalnih dijagnostičkih i terapeutskih agenasa za bolesti. Među bezbroj nanonosača, magnetne nanočestice (MNP) su izazvale veliko obećanje kao nove terapeutske primene jer ovi MNP mogu biti direktno ciljani na obolele ćelije sa efikasnom terapijskom efikasnošću. Za ovo, ovi MNP-ovi bi trebalo da budu modifikovani nekim visoko biokompatibilnim polimerima (posebno polisaharidima) koji pokazuju svojstva ciljanja raka, koja mogu snažno da interaguju sa receptorima eksprimiranim na ciljnom karcinomu kako bi se olakšalo tačno otkrivanje specifičnog raka i poboljšana isporuka na ciljno mesto uz smanjenje neželjene nuspojave. Tokom poslednjih nekoliko godina, mnoge grupe su prijavile hijaluronsku kiselinu (HA) kao sredstvo za ciljanje jer direktno isporučuje ciljane MNP u ćelije raka sa prekomernom ekspresijom CD44. U većini slučajeva, doksorubicin (DOKS) je korišćen kao lek protiv raka jer se u velikoj meri koristi za lečenje širokog spektra karcinoma. U našem radu, dizajnirali smo novu, intravenozno injekcionu, CD44 receptor ciljanu MNP formulaciju, gde HA deo MNP-a, olakšava lako otkrivanje ćelija raka putem interakcija specifičnih za receptor, DOKS može regresirati ćelije raka uz istovremenu efikasnost snimanja. Ovi teranostički MNP-i doveli su do formiranja nove nanoformulacije, sposobne da sprovede istovremenu detekciju, regresiju i snimanje u in vitro CD44 preko ekspresije ćelija raka.

Ključne reči: *multifunkcionalno, MNP, hijaluronska kiselina, doksorubicin, CD44.*

Naučni rad
Rad primljen: 28.09.2023.
Rad prihvaćen: 20.10.2023.
Rad je dostupan na sajtu: www.idk.org.rs/casopis